

Comparison of Partitioning of a Bimodal Polymer Mixture into Micropores in Good and Θ Solvents. A Monte Carlo Study

Peter Cifra,[†] Yongmei Wang,[‡] and Iwao Teraoka^{*,§}

Polymer Institute, Slovak Academy of Sciences, Dúbravská cesta 9, 842 36 Bratislava, Slovak Republic; Department of Chemistry, North Carolina A&T State University, Greensboro, North Carolina 27411; and Herman F. Mark Polymer Research Institute, Polytechnic University, 333 Jay Street, Brooklyn, New York 11201

Received June 4, 2001; Revised Manuscript Received October 18, 2001

ABSTRACT: We performed lattice Monte Carlo simulations to study partitioning of a mixture of short and long chains with a slitlike pore in good and Θ solvents, allowing unrestricted exchange of chains between the pore and the exterior solution. At high concentrations in the good solvent, the concentration of the short chains became higher in the pore than it was in the exterior. This partitioning inversion was not observed in the Θ solvent. The partition coefficients of the two components were nearly unchanged in the mixture as well as in solutions of pure polymer until the solution exterior to the pore reached the overlap concentration. The concentration that maximizes the resolution in size exclusion chromatography (SEC) shifted to a higher concentration in the Θ solvent. The purity of the short chains in the pore remained high over a wide range of concentrations. In contrast, the good solvent exhibited a drastic decrease in the purity as soon as the concentration increased slightly from zero. The comparison paves the way for potential operation of SEC at high concentrations in a Θ solvent. The concentration profiles of the two components in the slit always exhibited a deep depletion layer at the walls in the Θ solvent, different from the profiles in the good solvent that showed thinning of the depletion layer and segregation of the short chains near the walls. These differences are ascribed to $A_2 = 0$ or clustering of macromolecules in the Θ solvent.

Introduction

In recent years there has been growing interest in macromolecular systems confined in slitlike pores and their equilibria with the bulk. The interest is related to many industrial applications such as adhesion, lubrication, steric stabilization of colloids, flocculation, polymer intercalation in nanocomposites, novel surface apparatus, etc.^{1–5} Understanding the confinement effect is important in biological macromolecules and separation techniques such as gel electrophoresis, size exclusion chromatography (SEC), and membrane separation. The confinement can critically test thermodynamic theories of polymer. The principal mechanism in these applications is a loss of conformational entropy when confining a macromolecule to the slit.

Many of the studies on confined macromolecular systems used computer simulations.^{6–23} Most of them studied a confined region itself. Here we investigate a full equilibrium in which the free and the confined macromolecular solutions are in physical contact and coexist in a thermodynamic equilibrium.^{7,8,14,19–21} Our direct equilibrium of the two phases eliminates a need for chain insertion or deletion. The latter poses problems in dense polymer systems of long chains. Direct equilibration is possible due to a well-defined fixed geometry of the bulk/slit system.

We examine the effect of a variable solvent quality on the confined systems and on the partitioning with the confining geometry. We will show a different behavior in the Θ condition in comparison to the good solvent condition in the partitioning with a slit, first for monodisperse homopolymer and then for a mixture of

short and long chains. Finally, we investigate concentration profiles of these mixtures across the slit.

Characterization of macromolecules by SEC is performed typically in a good solvent. A concentration much lower than the overlap concentration is required for the solution injected into the column. A slight increase in the concentration distorts the chromatogram and leads to serious loss of resolution. We show here that use of Θ solvent as the mobile phase will tolerate a higher concentration in SEC. A novel method of separation of macromolecules at higher concentrations (high osmotic pressure chromatography, HOPC^{24,25}) can also be extended to higher concentrations in the Θ solvent compared with the good solvent.

Monte Carlo Simulations

The simulation procedure is described in papers devoted to the dimension and anisotropy of confined chains¹⁸ and to the modeling for chromatography at critical conditions.¹⁹ We assume two boxes connected to each other on a cubic lattice:¹⁴ the box E, representing the exterior (bulk) phase, and the box I, representing the interior slit pore. The box E has dimensions of $50a \times 30a \times 50a$ (a is the lattice unit) along the x , y , and z directions, respectively. In the box I of dimensions $(D + a) \times 30a \times 50a$, there are two solid walls at $x = a$ and $x = D + a$ extending in the y and z directions, thereby forming a slit. The width D is defined as the distance between the two lattice layers occupied by the solid walls. The polymer beads are not allowed to occupy the sites on the solid walls. Periodic boundary conditions apply to all pairs of opposite walls in the boxes except the solid walls.

The self-avoiding walks consisting of N beads in each chain were generated on the cubic lattice. We used $N = 100$ for homopolymer solutions and $N_L = 20$ and $N_H =$

[†] Slovak Academy of Sciences.

[‡] North Carolina A&T State University.

[§] Polytechnic University.

Table 1. Coil-to-Pore Size Ratio in Slit of $D/a = 6$

chain	solvent	$\lambda = 2R_{g0}/D$
$N_L = 20$	good	0.803
	Θ	0.744
$N_H = 100$	good	2.15
	Θ	1.78

Table 2. Overlap Concentration ϕ^*

composition	good solvent	Θ solvent
$N = 100$ only	0.120	0.207
$N = 100$ and 20 in 1:1	0.185	0.291

100 for mixtures, where N_L and N_H denote the numbers of beads in the shorter and longer chains, respectively. The athermal model with zero value of the reduced contact energy $\epsilon_s = \epsilon_s/kT$, where ϵ_s is the segment-segment contact energy and kT the thermal energy, represents the good solvent condition. The restrictions on the lattice occupancy bring about the volume expansion of the chain segments resembling that of polymer chains in good solvents. The Θ chains were generated by using $\epsilon_s = -0.2693$ for both intra- and intermolecular nonbonded contacts as discussed earlier.^{17,23,26} In the mixture at the Θ state, all three interactions, including the cross interaction, must assume the same value of ϵ_s between nonbonded contacts, i.e., $\epsilon_{LL} = \epsilon_{HH} = \epsilon_{LH} = -0.2693$, where ϵ_{ij} stands for the interaction between monomers of components i and j ($i, j = L$ for short chains and H for long chains).

Chains were equilibrated by using the reptation moves and the Metropolis algorithm. Unrestricted exchange of chains between the bulk and the slit gave the equilibrium concentrations without a need to calculate the confinement free energy from the respective chemical potentials. The respective final concentrations are the results of equilibration for all the chains in the system. The ratio of the volume fractions of the polymer in boxes I and E at equilibrium, ϕ_I/ϕ_E , gives the partition coefficient K . The chains in the intermediate regions with their parts belonging to both boxes I and E contributed all their segments either to ϕ_I or to ϕ_E , depending on where the majority of the chain segments is located. Concentrations up to $\phi_E = 0.7$ were used. For the mixture of short and long chains, a 1:1 composition in volume fractions was used. The mixture composition in box E was nearly unaltered by the partitioning because of excess volume of box E compared to box I for the narrow slit used in the present study. The composition changes slightly for broader slits. Simulations of pure polymer were performed for the range of slit width of $D/a = 6$ –46. For mixtures, the slit width was $D/a = 6$ for the partitioning studies and 8 for the concentration profiles. The coil-to-pore size ratio, defined as $\lambda = 2R_{g0}/D$, ranged between 0.744 and 2.15 depending on the chain length and solvent quality and is listed in Table 1. Here R_{g0} is the root-mean-square radius of gyration of the chain in the low concentration limit in the exterior phase. These ranges are typical in experimental partitioning studies.

The overlap concentration ϕ^* is listed in Table 2 for pure polymers of $N = 100$ and a 1:1 mixture of $N_L = 20$ and $N_H = 100$ in the good solvent and the Θ solvent. For the pure polymer, $\phi^* = N/(2^{1/2}(R_{g0}/a + \alpha))^3$, where $\alpha = 0.199$ for the good solvent and 0.204 for the Θ solvent.^{16,17} For the 1:1 mixture, $\phi^* = 2/[(2^{1/2}(R_{g0H}/a + \alpha))^3/N_H + 2^{1/2}(R_{g0L}/a + \alpha)^3/N_L]$, where R_{g0H} and R_{g0L} are the radii of gyration for the two components.

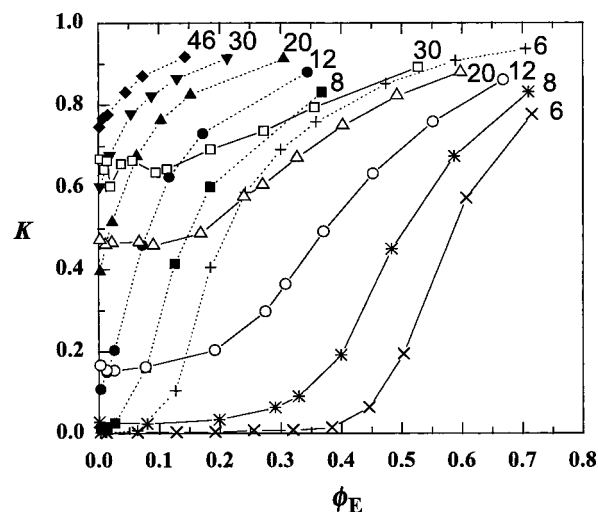


Figure 1. Partition coefficient K of pure polymer of $N = 100$ with slits of different widths, plotted as a function of concentration ϕ_E in the exterior solution. Dotted lines are for the good solvent, and solid lines are for the Θ solvent. The slit width D/a is indicated adjacent to each curve.

Results and Discussion

Partitioning of Pure Polymer Solutions. Before investigating the partitioning for the mixture, it is instructive to look at the partitioning for the pure polymer solutions. Figure 1 presents the results for the partition coefficient K . The slit-to-pore size ratio λ ranges between 0.28 and 2.15 for athermal solutions and between 0.36 and 1.78 for Θ solutions. In the good solvent, an increase in concentration ϕ_E leads immediately to a stronger penetration of the chains into the slit. This phenomenon was described as a weak-to-strong penetration transition.^{3,14} The behavior of Θ chains is different. The penetration transition is held back to higher concentrations. The partition coefficient does not increase until ϕ_E reaches ϕ^* even in the widest slit. The zero concentration dependence at low concentrations is explained by the missing second virial coefficient, $A_2 = 0$. Microscopically, this phenomenon is related to a clustering of chains at Θ conditions¹⁷ as a result of proximity to polymer-solvent demixing. This delayed transition was described by the scaling approach¹⁷ similar to the one that explained the transition for the good solvent.¹⁴ Figure 1 contains the data we obtained earlier¹⁷ and additional data for the more strongly confining slit, $D/a = 6$.

We can use the series of curves in Figure 1 obtained for different slit widths but a fixed chain length of $N = 100$ to estimate the partitioning characteristics for chains of another length. The partition coefficient of the chain in the low concentration limit is found by comparing its value of $2R_{g0}/D$ with the values listed for $N = 100$. The transition characteristics depend primarily on ϕ_E/ϕ^* for a given solvent quality, because the increase in K is dictated by the excess chemical potential that primarily depends on ϕ_E/ϕ^* . In the mean-field theory for confined athermal chains,²² the partitioning depends on R_{g0}/D and ϕ_E/ϕ^* only. In the Θ condition,²⁷ it is also the case for sufficiently long chains. Thus, Figure 1 can be viewed as a universal plot that gives an estimate of K for a given coil-to-pore size ratio at a given ϕ_E (or ϕ_E/ϕ^*).

Partitioning of Mixture Solutions. Earlier we investigated the partitioning for a bimodal mixture of

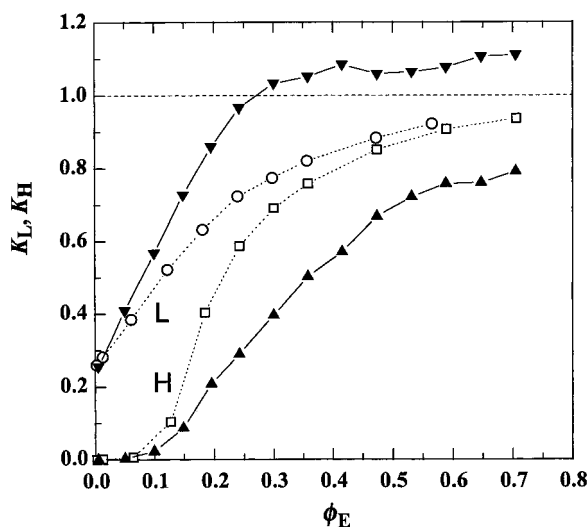


Figure 2. Partition coefficients K_L and K_H of short (L) and long (H) chains ($N_L = 20$ and $N_H = 100$) in the good solvent with a slit of width $D/a = 6$, plotted as a function of ϕ_E . The solid lines are for the mixture, and the dotted lines are for the pure polymer solutions. The mixture has the two components at equal volume fractions.

long and short chains ($N_L = 25$ and $N_H = 100$) in the good solvent with a slit of $D/a = 9$.²⁰ Here we compare mixtures consisting of chains with $N_L = 20$ and $N_H = 100$ at a volume composition of 1:1 in the good solvent and the Θ solvent to elucidate the effect of thermodynamic quality of the solvent on the partitioning.

a. Good Solvent. Solid lines in Figure 2 show the partition coefficients K_H and K_L of the long and short chains in the mixture as a function of the total volume fraction of chains, ϕ_E , in the exterior solution. For reference, the partition coefficients of the two chains in their respective pure solutions are shown as dashed lines. The slit width is $D/a = 6$. At low concentrations, the partitioning is determined by R_{g0}/d for each chain. Thus, K does not depend on whether the partitioning macromolecule is in the mixture or in the pure polymer. The two curves for the pure polymer and the respective component in the mixture have the same value at $\phi_E = 0$. At higher concentrations we start to see a difference. The long chains in the mixture experience repulsion by the short chains that enter the slit more easily. The mixture has therefore a smaller K_H compared with the pure polymer. Concurrently, the short chains are expelled into the pore by congested long chains in the exterior solution. Therefore, K_L in the mixture exceeds the one in the pure polymer. At even higher concentrations the partitioning inversion²⁵ ($K_L > 1$) is observed, in which the short chains have a higher concentration in the confined region compared with the exterior solution.

Apparently, the universality of Figure 1 fails in the mixture. We see a different shape of the curve for short and long chains in Figure 2. Rescaling the abscissa does not overlap either curve with any dotted line in Figure 1.

b. Θ Solvent. Adoption of the attractive interactions $\epsilon_{LL} = \epsilon_{HH} = \epsilon_{LH} = -0.2693$ that represent the Θ condition significantly changes the partitioning. Figure 3 depicts the results for the Θ mixture. Both curves start with a near-zero slope, indicating that both components are at the near- Θ condition. At low concentrations the partition coefficient starts from the same values of K

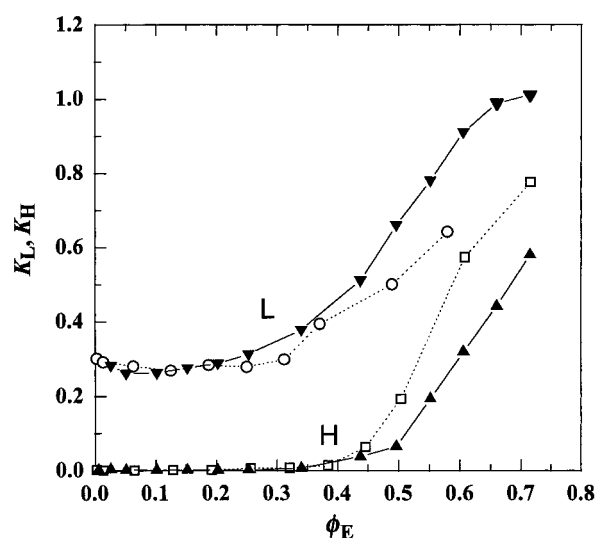


Figure 3. Partition coefficients K_L and K_H of short (L) and long (H) chains ($N_L = 20$ and $N_H = 100$) in the Θ solvent with a slit of width $D/a = 6$, plotted as a function of ϕ_E . The solid lines are for the mixture, and the dotted lines are for the pure polymer solutions.

irrespective of whether the chains belong to the mixture or to the pure polymer. The partition coefficient remains nearly unchanged over a wide range of concentrations in solution of pure polymer as well as in solution of the mixture. A slight decrease in K_L suggests that the interaction of -0.2693 causes a slightly negative A_2 . Stronger penetration of components into the slit with an increasing ϕ_E is delayed to a much higher concentration (at around ϕ^*) for the mixture in comparison to the good solvent. At higher concentrations, first K_L and then K_H start to rise. Compared with the pure polymer at the same concentration, K_L is larger and K_H is smaller. The difference, however, is smaller than it is in the good solvent. The short chains that crowd the pore expel the long chains, but to a lesser extent compared with the good solvent. The partitioning inversion that was seen in the good solvent does not appear here except the highest concentration.

To examine the partitioning of the mixture quantitatively, we plot $K_L - K_H$ in Figure 4 and K_L/K_H in Figure 5, both as a function of ϕ_E . The results for the good solvent and the Θ solvent are compared.

In Figure 4, $K_L - K_H$ represents a resolution of SEC for given confinement and mixture parameters. Note that the peak retention time in chromatography is a linear function of the partition coefficient. A greater difference between K_L and K_H gives a better separation. In the Θ solvent, $K_L - K_H$ is nearly flat in the range of $\phi_E < \phi^*$, in a stark contrast to the good solvent in which $K_L - K_H$ increases as soon as ϕ_E increases slightly from zero. The peak in the plot is shifted to a higher concentration of $\phi_E \approx 0.55$ in the Θ solution from its position at $\phi_E \approx 0.2$ in the good solvent. Earlier, we noted that the peaking in $K_L - K_H$ in the good solvent gives the optimal separation condition for HOPC.²⁰ In the Θ solvent, HOPC can be operated at even higher concentrations. The processing capacity of HOPC is therefore higher in the Θ solvent.

In Figure 5, the ratio represents a purity of the short chains in the pore. The high ratio indicates a high purity. The concentration range with $K_L/K_H > 10$ is limited to $\phi_E < 0.15$ in the good solvent but extends to $\phi_E = 0.4$ in the Θ solvent.

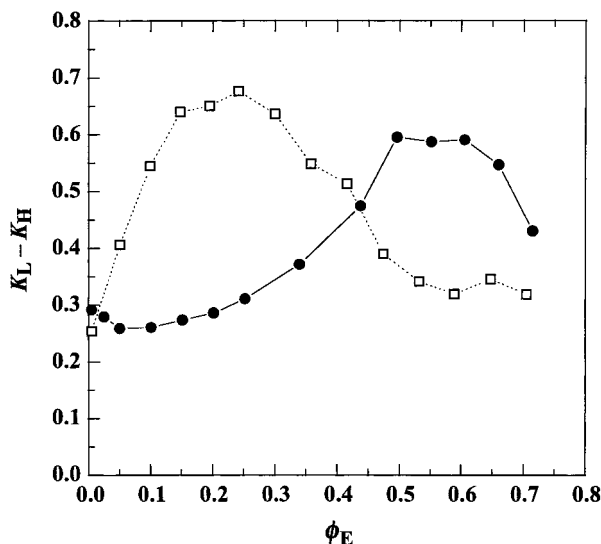


Figure 4. Difference in the partition coefficients, $K_L - K_H$, is plotted as a function of ϕ_E in the good solvent (dotted line) and the Θ solvent (solid line).

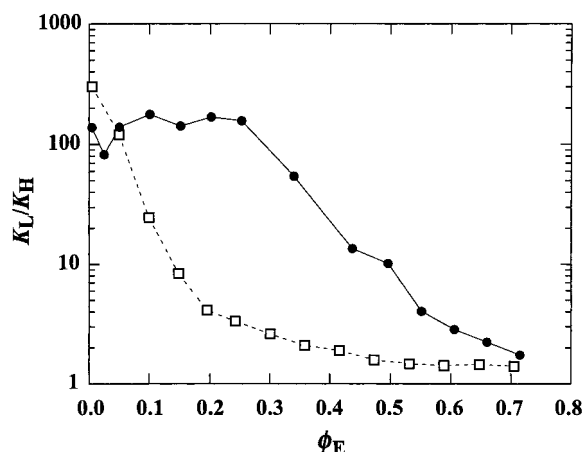


Figure 5. Ratio of the partition coefficients, K_L/K_H , is plotted as a function of ϕ_E in the good solvent (dashed line) and the Θ solvent (solid line).

A wide range of nearly constant partition coefficients in the Θ solvent indicates that, if one uses as a mobile phase a Θ solvent for the polymer in an SEC analysis, the chromatogram will be almost unchanged over a wide range of injected solution concentrations. Then, one can effectively use higher concentrations without being compromised by the problem of overloading. The high loading will facilitate detection of a smaller sample volume and therefore pave the way for miniaturization of chromatographic separation systems.

We note here that the high ratio of K_L/K_H at high concentrations in the equilibrium between two boxes E and I of comparable volumes is important, because the situation resembles that of the partitioning in the chromatographic column in HOPC. The high ratio at high concentrations means a high purity of the long chains in the exterior. For this purpose, we need to conduct simulations for the comparable volumes. The exterior solution will be away from 1:1 composition.

A better separation of the mixture by the confinement in the Θ solvent is related to a similar effect occurring at polymer interfaces. A surface segregation in the polymer mixture, or wetting of surface by an extensive layer, is enhanced when the polymer mixture is brought

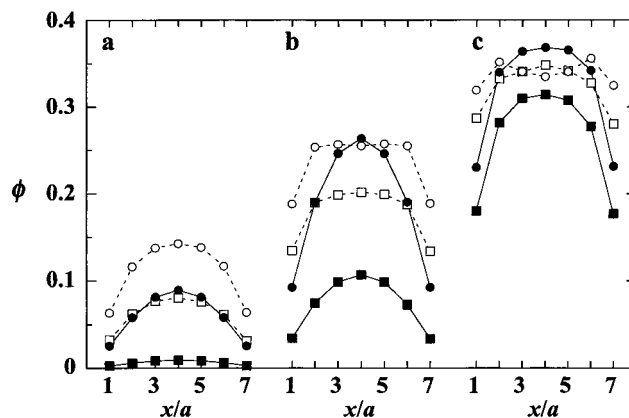


Figure 6. Concentration profiles of short chains (circles) and long chains (squares) in a slit of width $D/a = 8$ in the good solvent (dotted lines) and Θ solvent (solid lines). The total concentration ϕ_E in the exterior solution in the three parts is given in Table 3.

Table 3. Average Concentrations

figure	solvent	ϕ_E	$\phi_I(L)$	$\phi_I(H)$
a	good	0.2339	0.1113	0.0601
	Θ	0.2480	0.0599	0.0063
b	good	0.4785	0.2364	0.1781
	Θ	0.4579	0.1888	0.0743
c	good	0.6919	0.3381	0.3224
	Θ	0.6815	0.3200	0.2639

closer to the phase separation.²⁸ We will discuss the surface segregation again in the following section.

Concentrations Profiles of the Mixture. Concentrations profiles of confined polymer have a relevance to many applications and provide a good test of thermodynamic theories.²⁷ Three parts of Figure 6 compare the concentration profiles of the two components in the good and Θ solvents in a slit of $D/a = 8$, slightly broader than the one used in the preceding figures. A pair of simulation results that have a similar ϕ_E were selected for comparison. Table 3 lists ϕ_E and the average concentrations $\phi_I(L)$ and $\phi_I(H)$ of the two components in the pore for the three parts of the figure. Part a shows typical profiles for the dilute solutions with no plateau in the middle of the slit and depletion at the slit walls in the good solvent and the Θ solvent, indicating strong confinement for both components.

In part b, the profiles are greatly different between the two solvents. As already seen in the pure polymer,¹⁸ the good solvent is able to fill up the depletion layer better than the Θ solution does. The profiles in the good solvent has another feature: a segregation of short chains toward the walls. We see a local maximum in the concentration profile near the walls. In the Θ solvent, the profiles are still nearly the same as those in part a.

With a further increase in ϕ_E (part c), the monomers spread even more closely to the walls in the good solvent. The surface segregation of the short chains is more pronounced, exhibiting a deeper and broader dip in the profile of the short chains compared with the one in part b. In the Θ solvent, in contrast, there is no dip in the profile. The depletion layer at the slit walls still exists. This observation confirms already reported surface segregation in athermal mixture at the walls.²⁹ In the Θ solvent, the concentration profiles are almost identical between the short and long chains except for the absolute height. In fact, the six profiles in the Θ solvent in the three parts of the figure stack on top of

each other (not shown). It is difficult to tell which one is for the short chains.

We note here that the ratio of the concentration of the short chains in the layers next to the walls to that of the long chains is consistently higher in the Θ solvent than it is in the good solvent. It is the case at all concentrations including those shown in the three parts of Figure 6. The Θ solvent is more effective in enriching the short chains at the walls.

The observation also indicates that partitioning of the mixture into the pore is affected by the surface segregation in mixture. The theoretical treatment for the partitioning of a mixture needs to take the surface segregation into account. A formulation that neglects the segregation does not provide a correct account of the partitioning characteristics.^{14,30}

Conclusions

We conducted lattice simulations on the partitioning of a mixture of short and long chains with a slit to show that the Θ solvent as a mobile phase is a viable option for the chromatographic separation. We pointed out that the resolution and the processing capacity can be higher in size exclusion chromatography and high osmotic pressure chromatography (HOPC) when the Θ solvent is used compared with the good solvent. We are currently comparing the performance of HOPC for polycaprolactone in a good solvent (dioxane) and in a near- Θ solvent (toluene) conditions. We could successfully avoid adsorption by employing a stationary phase that repels the polymer even in the Θ solvent. The resolution is much better in the Θ condition. We are also conducting study of regular SEC in the Θ condition.

Our simulation was performed for one combination of the two chain lengths and a mixture of equal volume fractions only. The simulation needs to be performed for different chain length ratios, slit widths, and mixing ratios. Furthermore, the relatively short chains adopted in the present study did not allow us to reach a concentration several times as high as the overlap concentration before the monomer concentration becomes too high.

Acknowledgment. The authors acknowledge support from NSF-DMR-9876360. P.C. acknowledges support by the Grant Agency for Science (VEGA), Grant

2/7076/21. The use of computer resources of the Computing Center of SAS and of North Carolina Supercomputer Center is gratefully acknowledged.

References and Notes

- (1) Fleer, G. J.; Cohen-Stuart, M. A.; Scheutjens, J. M. H. M.; Cosgrove, T.; Vincent, B. *Polymers at Interfaces*; Chapman & Hall: London, 1993.
- (2) Sanchez, I. C., Ed.; *Physics of Polymer Surfaces and Interfaces*; Butterworth-Heinemann: Boston, 1992.
- (3) Daoud, M.; de Gennes, P. G. *J. Phys. (Paris)* **1977**, *38*, 85.
- (4) Raphael, E.; Pincus, P. *J. Phys. II* **1992**, *2*, 1341.
- (5) Casassa, E. F. *J. Polym. Sci., Polym. Lett. Ed.* **1967**, *5*, 773.
- (6) Shih, W. Y.; Shih, W.-H.; Aksay, I. A. *Macromolecules* **1990**, *23*, 3291.
- (7) Yethiraj, A.; Hall, C. K. *Mol. Phys.* **1991**, *73*, 503.
- (8) Vacatello, M.; Auriemma, F. *Macromol. Chem. Theory Simul.* **1993**, *2*, 77.
- (9) van Vliet, J. H.; Luyten, M. C.; ten Brinke, G. *Macromolecules* **1992**, *25*, 3802.
- (10) Kumar, S. K.; Vacatello, M.; Yoon, D. Y. *Macromolecules* **1990**, *23*, 2189.
- (11) Lee, J. Y.; Baljon, A. R. C.; Loring, R. F.; Panagiotopoulos, A. Z. *J. Chem. Phys.* **1998**, *109*, 10321.
- (12) Milchev, A.; Binder, K. *Eur. Phys. J. B* **1998**, *3*, 477; **2000**, *13*, 607.
- (13) De Joannis, J.; Jimenez, J.; Rajagopalan, R.; Bitsanis, I. *Europhys. Lett.* **2000**, *51*, 41.
- (14) Wang, Y.; Teraoka, I. *Macromolecules* **1997**, *30*, 8473.
- (15) Cifra, P.; Bleha, T. *Macromol. Theory Simul.* **1999**, *8*, 603.
- (16) Wang, Y.; Teraoka, I. *Macromolecules* **2000**, *33*, 3478.
- (17) Cifra, P.; Bleha, T.; Wang, Y.; Teraoka, I. *J. Chem. Phys.* **2000**, *113*, 8313.
- (18) Cifra, P.; Bleha, T. *Macromol. Theory Simul.* **2000**, *9*, 555.
- (19) Cifra, P.; Bleha, T. *Polymer* **2000**, *41*, 1003.
- (20) Wang, Y.; Teraoka, I.; Cifra, P. *Macromolecules* **2001**, *34*, 127.
- (21) Cifra, P.; Bleha, T. *Macromolecules* **2001**, *34*, 605.
- (22) Teraoka, I.; Wang, Y. *J. Chem. Phys.* **2001**, *115*, 1105.
- (23) Dickman, R. *J. Chem. Phys.* **1992**, *96*, 1516.
- (24) Teraoka, I. In *Column Handbook for Size Exclusion Chromatography*; Wu, C.-S., Ed.; Academic Press: San Diego, 1999.
- (25) Teraoka, I.; Zhou, Z.; Langley, K. H.; Karasz, F. E. *Macromolecules* **1993**, *26*, 3223.
- (26) Panagiotopoulos, A. Z.; Wong, V.; Floriano, M. A. *Macromolecules* **1998**, *31*, 912.
- (27) Teraoka, I.; Cifra, P. *J. Chem. Phys.*, in press.
- (28) Schmidt, I.; Binder, K. *J. Phys. (Paris)* **1985**, *46*, 1631.
- (29) Hariharan, A.; Kumar, S. K.; Russel, T. P. *Macromolecules* **1990**, *23*, 3584.
- (30) Teraoka, I.; Langley, K. H.; Karasz, F. E. *Macromolecules* **1993**, *26*, 287.

MA010963Y